

## Supplementary information

### Contribution of nitrated phenols to wood burning brown carbon light absorption in Detling, UK during winter time

*Claudia Mohr<sup>1</sup>, Felipe D. Lopez-Hilfiker<sup>1</sup>, Peter Zotter<sup>2</sup>, André S. H. Prévôt<sup>2</sup>, Lu Xu<sup>3</sup>, Nga. L. Ng<sup>3</sup>, Scott C. Herndon<sup>4</sup>, Leah R. Williams<sup>4</sup>, Jonathan P. Franklin<sup>4</sup>, Mark S. Zahniser<sup>4</sup>, Douglas R. Worsnop<sup>4,5</sup>, W. Berk Knighton<sup>6</sup>, Allison C. Aiken<sup>7</sup>, Kyle J. Gorkowski<sup>7,8</sup>, Manvendra K. Dubey<sup>7</sup>, James D. Allan<sup>9</sup>, and Joel A. Thornton<sup>1\*</sup>*

<sup>1</sup>Department of Atmospheric Sciences, University of Washington, Seattle WA 98195

<sup>2</sup>Paul Scherrer Institute, Laboratory for Atmospheric Chemistry, Villigen 5232, Switzerland

<sup>3</sup>Georgia Institute of Technology, School of Earth and Atmospheric Sciences, Atlanta GA 30332

<sup>4</sup>Aerodyne Research, Inc., Billerica MA 01821

<sup>5</sup>Department of Physics, University of Helsinki, Helsinki, Finland

<sup>6</sup>Department of Chemistry and Biochemistry, Montana State University, Bozeman MT 59717

<sup>7</sup>Los Alamos National Laboratory, Earth and Environmental Sciences Division, Los Alamos NM 87545

<sup>8</sup>Now in Civil and Environmental Engineering, Carnegie Mellon University, Pittsburgh PA 15213

<sup>9</sup>National Centre for Atmospheric Science & School of Earth, Atmospheric and Environmental Sciences, University of Manchester, Manchester M13 9PL, UK

\*Corresponding author email: [thornton@atmos.uw.edu](mailto:thornton@atmos.uw.edu), phone: +1 206-543-4010

Number of pages: 10

Number of figures: 10

Nr of tables: 1

## 1. ClearLo field site, Detling, UK

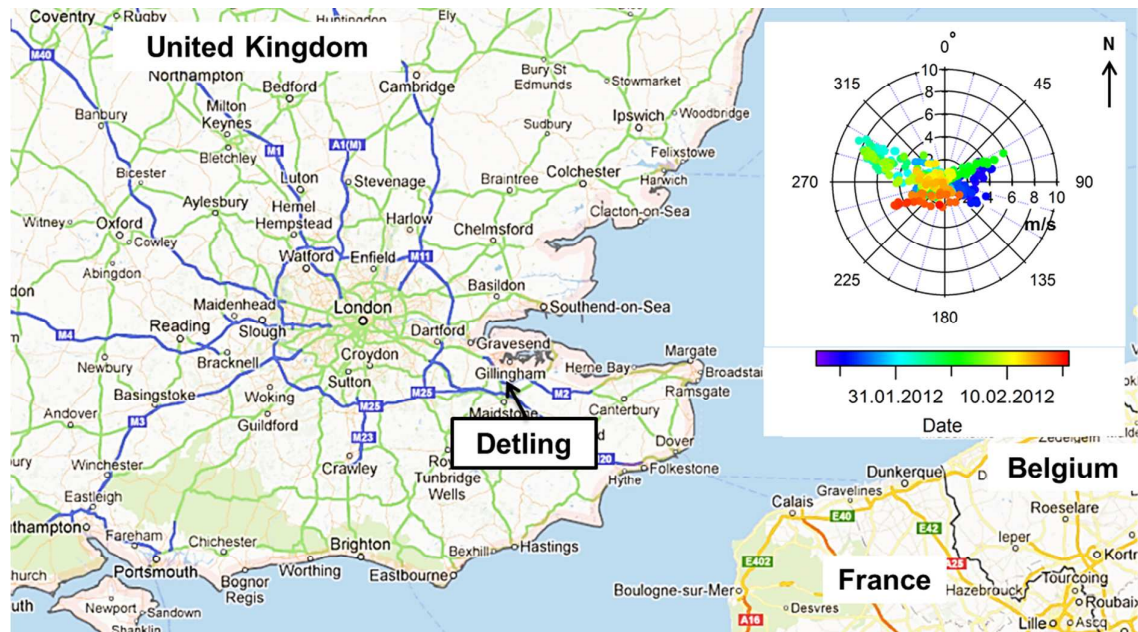


Figure S 1: Map of the location of Detling UK, with southeastern UK, the English Channel and northwestern continental Europe. The wind rose in the upper right corner shows the wind directions and wind speeds during the ClearLo campaign.

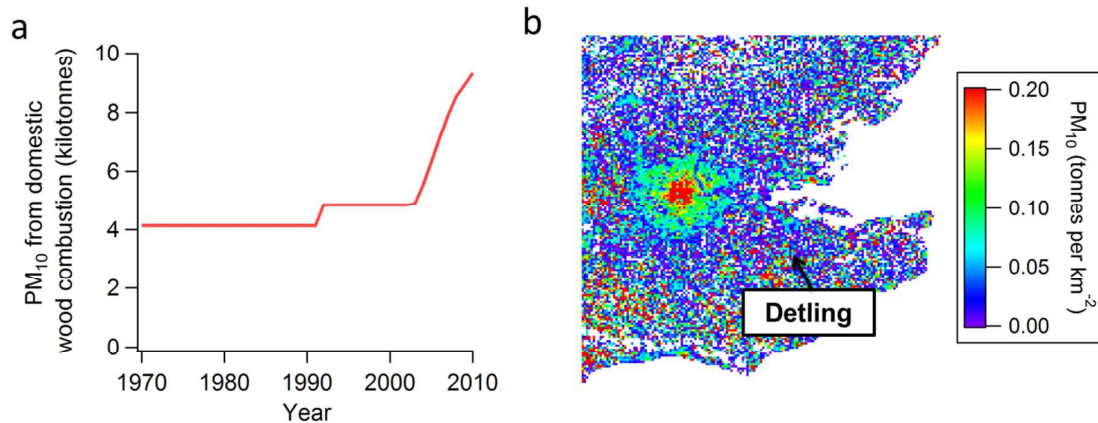


Figure S 2: Development of the kilotonnes of PM<sub>10</sub> emitted by domestic wood burning activities since 1970 (a) and the spatial distribution of PM<sub>10</sub> (kilotonnes) in 2010 from commercial, institutional, residential and agriculture sectors, excluding point sources (b). Data source: <http://naei.defra.gov.uk>.<sup>1</sup>

## 2. Declustering conditions

The average E/N (electric field divided by the number density) between the CDC and the back Q2 regime was 390 Td, the mean acetate dimer ( $\text{CH}_3\text{C}(\text{O})\text{OH}$ ).( $\text{CH}_3\text{C}(\text{O})\text{O}^-$ ) to monomer ( $\text{CH}_3\text{C}(\text{O})\text{O}^-$ ) ratio was 0.07, the acetic anhydride flow was 50 sccm and the total IMR flow was  $4.5 \text{ l m}^{-1}$  during the ClearLo campaign.

## 3. Measurement cycles during ClearLo and gas phase calibrations

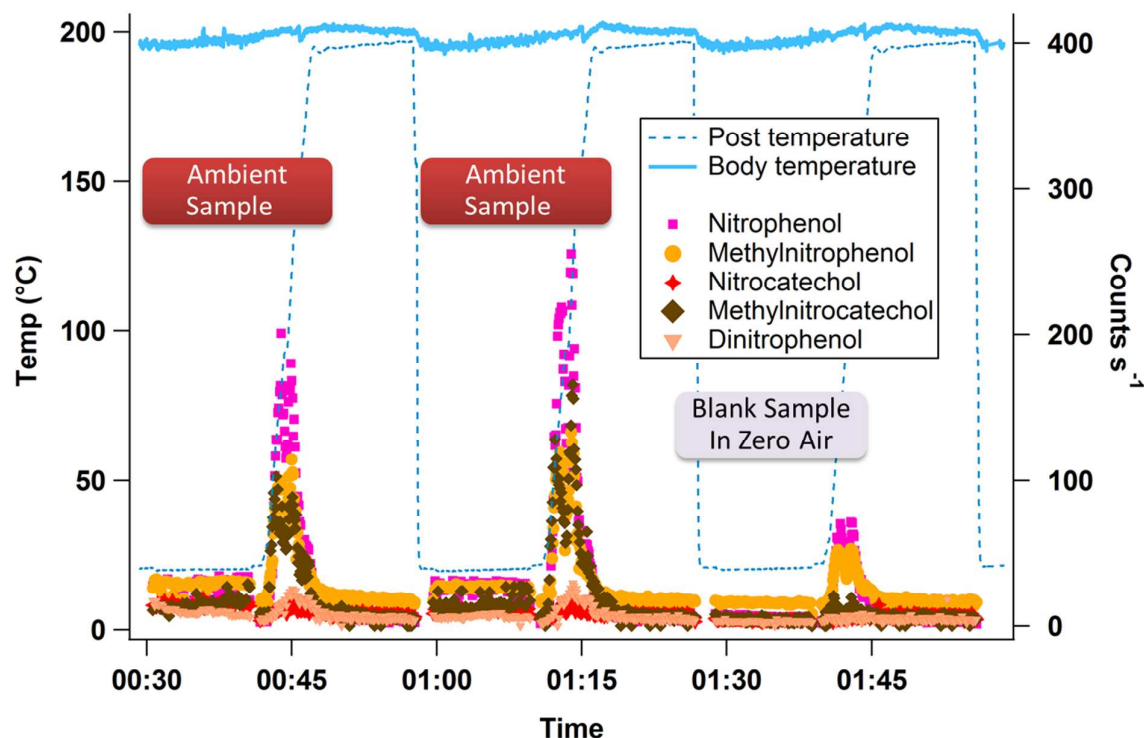


Figure S 3: Measurement cycle, negative mode only, of the MOVI during the ClearLo measurements in Detling, UK.

Zero air was generated with a Zero air generator (Teledyne, USA) for blanks. Calibration gas (formic acid) was added during the sampling and blank phases for 2 minutes at random instants of time at the top of the inlet (not shown). We used a permeation tube of formic acid kept at  $70 \text{ }^\circ\text{C}$ , with an emission rate of  $120 \text{ ng min}^{-1}$ .

## 4. Quantifications of nitrated phenols

The sensitivity of the MOVI-HRToF-CIMS to nitrated phenols was determined in the laboratory after the campaign by injecting known quantities (in solution) into the MOVI, within 1 mm of the impaction post using a microliter syringe (Hamilton, USA). The MOVI and IMR conditions were identical to those in the campaign. Solutions of 4-Methyl-2-nitrophenol (4M2NP, 99%), 4-Nitrocatechol (4NC, 97%), 2-Nitrophenol (2NP, 98%), and 4-Nitrophenol (4NP, not specified) were prepared in acetone with concentrations in the range of  $\mu\text{mol/l}$  for all compounds except 4NP ( $\text{nmol/l}$ ). Nitroaromatics were purchased from Sigma Aldrich and used without further purification.

Acetone was chosen as the solvent primarily because of its aprotic nature to avoid hydrolysis or other solution chemistry. Amounts of 2  $\mu\text{l}$ , 5  $\mu\text{l}$ , 10  $\mu\text{l}$ , 15  $\mu\text{l}$ , and 20  $\mu\text{l}$  were delivered to the MOVI using a syringe (Hamilton, USA). The resulting data peaks were integrated, yielding a total ion counts signal per injection, which was plotted versus the amount of compound delivered in ng per injection, showing a linear relation. The signal pulses arising from injections were time integrated and demonstrated linearity ( $R^2 \geq 0.95$ ) and reproducibility across the concentration range used (see Figure S4).

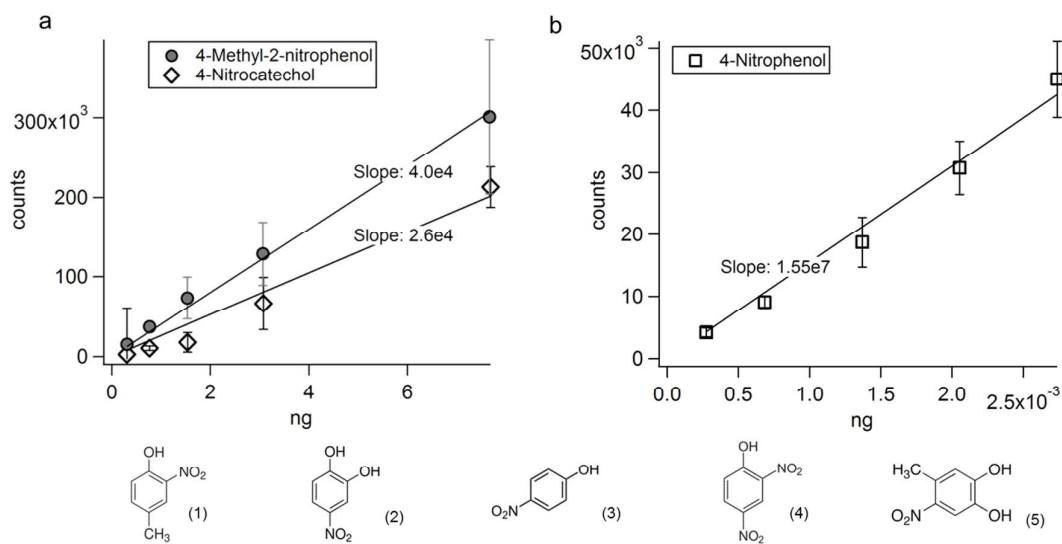


**Figure S 4: Calibration curves of 4-Methyl-2-nitrophenol, 4-Nitrocatechol (a), and 4-Nitrophenol (b). The slopes represent the sensitivities in counts ng<sup>-1</sup> used for the quantification of the NAs measured in Detling. The skeletal formulas depict tentative structures of the nitrated phenols compounds measured and quantified with the CIMS in Detling: (1) Methylnitrophenol, (2) nitrocatechol, (3) nitrophenol, (4) dinitrophenol, and (5) methylnitrocatechol. The error bars represent  $\pm 1$  standard deviation.**

## 5. ClearLo mean diurnal pattern of NO<sub>x</sub> and CO

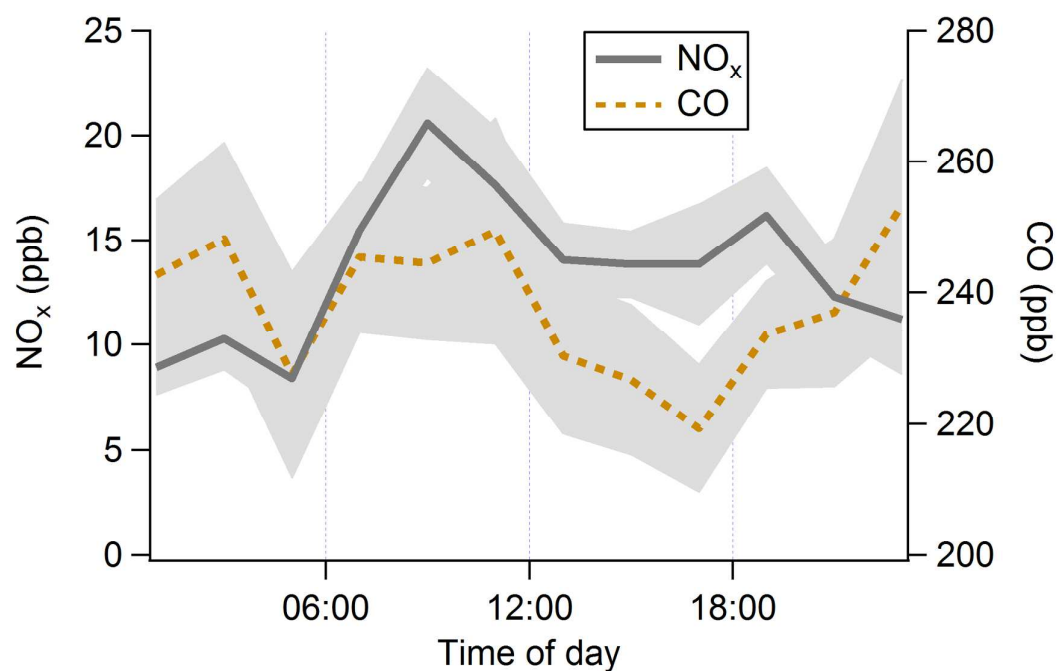


Figure S 5: Campaign average diurnal pattern of CO and NO<sub>x</sub> as measured in Detling, UK during the ClearLo campaign. The shaded grey areas represent  $\pm$  the standard error of the mean.

## 6. Positive Matrix Factorization PMF

**Pretreatment of data.** Positive Matrix Factorization (PMF) was performed on unit mass resolution (UMR) organics spectra. The PMF2 executable version 4.2 in the roust mode<sup>2</sup>) and PMF Evaluation Toolkit (PET) introduced by Ulbrich et al.<sup>3</sup> were used to process the data. Organic mass spectra matrix was generated using the “fragmentation table” technique<sup>4</sup> and errors matrix was generated following the procedures described by Ulbrich et al.<sup>3</sup> Any  $m/z$ 's with  $0.2 < \text{signal-to-noise (SNR)} < 2$  are considered “weak” and downweighted by a factor of 2, and  $m/z$ 's with SNR smaller than 0.2 are considered “bad” and removed to reduce disproportionate effects on the fitting outcome. In order to prevent excessive weighting of the  $m/z = 44$  variable, the signals at  $m/z = 16, 17, 18, 44$  were downweighted before PMF.

**Choice of number of factors.** PMF was run under a range of number of factors ( $P$ ). The three factor solution was chosen after carefully examining the total sum of the squares of the scaled residual ( $Q_{\text{value}}$ ), factor correlation with external tracers (including CH<sub>3</sub>CN, NO<sub>x</sub>, NO<sub>3</sub>), and signs of “split” of factors, which were described by Zhang et al.<sup>5</sup>

**Rotational ambiguity or numerical stability.** The rotational ambiguity was checked by changing the parameter FPEAK. Improved correlations with external tracers were not found for FPEAK values different from 0. Therefore, a FPEAK value of 0 was used for the solution. The robustness of the solution was examined by running PMF with different initial conditions (SEED parameter, pseudorandom value from which to start the PMF algorithm to explore possible local minima of the  $Q_{\text{value}}$ ), and all three factors were remarkably stable across different solutions.

## 7. MOVI-HRToF-CIMS mass spectrum

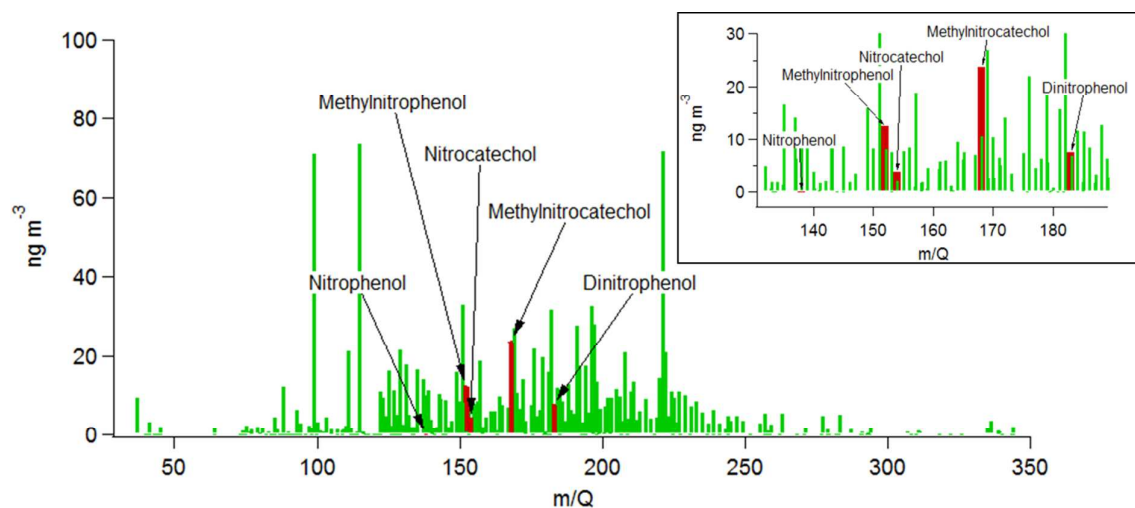


Figure S 6: Mass spectrum (organic compounds only) from February 4 shortly after midnight, integrated over one heating cycle and background subtracted. Mass concentrations are calculated based on gas phase formic acid sensitivity ( $8.9 \times 10^6$  counts  $\text{nmol}^{-1}$ ). The nitrated phenols are highlighted in red; their mass concentrations have been calculated based on NA calibrations in the laboratory. The inset shows a zoom of the m/Q region of the nitrated phenols.

## 8. Correlation coefficient of individual NA compounds and AMS-PMF factors

Table S 1: Correlation coefficients of the five individual NA compounds and the AMS-PMF factors. The highest values per compound are highlighted

Pearson's $r(293)$ , $p < 0.05$	NP	MNP	NC	MNC	DNP
BBOA	<b>0.52</b>	<b>0.56</b>	<b>0.66</b>	<b>0.53</b>	0.40
HOA	0.30	0.31	0.47	0.29	0.21
OOA	0.42	0.25	0.46	0.17	<b>0.60</b>

## 9. CO background determination

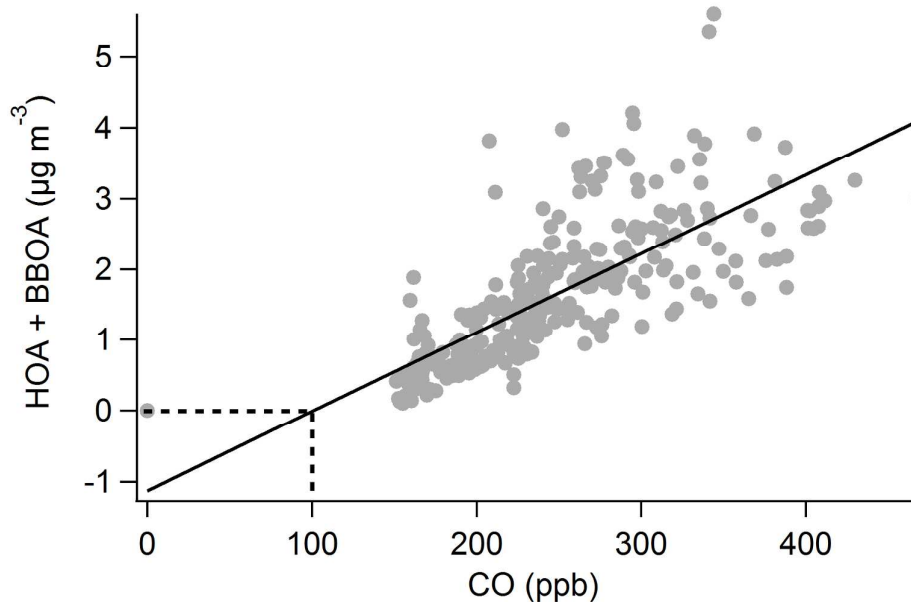


Figure S 7:  $\Delta\text{CO}$  equals CO minus a CO background, which was determined to be 100 ppb for this dataset based on the x-axis intercept of the (HOA + BBOA) to CO regression analysis.

## 10. Diurnal pattern of dinitrophenol/nitrophenol

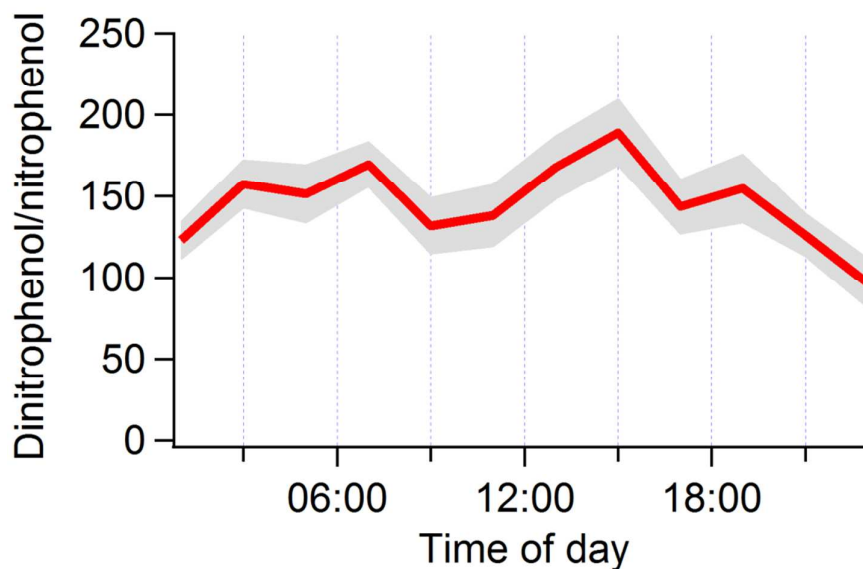


Figure S 8: ClearfLo campaign average diurnal pattern of the ratio of dinitrophenol ( $\text{ng m}^{-3}$ ) and nitrophenol ( $\text{ng m}^{-3}$ ). The shaded grey areas represent  $\pm$  the standard error of the mean.

## 11. Separation of $b_{\text{abs}}$ into OC/BC and wood burning/traffic fractions

Figure S9 shows the average  $b_{\text{abs}}$  per  $\lambda$  measured with the aethalometer for Detling (red dots). The power law fit yields an  $\alpha$  of 1.7. Kirchstetter et al.<sup>6</sup> recently used data from the 7-wavelength

aethalometer to estimate the contribution to light absorption from OC and BC. The BC fraction was calculated using  $\alpha = 0.86$ , and the difference of total attenuation and BC attenuation was assigned to OC attenuation. Values close to 1 have been shown to represent well the light-absorbing behavior of freshly emitted BC,<sup>7-9</sup> whereas  $\alpha$  values for wood burning generated particulate matter exhibit a broader range greater than 1<sup>6, 7, 10</sup> and are usually assigned to non-BC or light absorbing organic matter termed brown carbon. The same concept applied to the aethalometer data from Detling and using  $\alpha = 1$  for the BC fraction yielded an  $\alpha$  value of 2.2 for the organic (brown carbon) fraction (Figure S9). A similar concept, based on the Beer-Lambert's law, aethalometer  $b_{abs}$  measurements at two different wavelengths, and different  $\alpha$  values for traffic and wood burning (WB) carbonaceous matter absorption, respectively, was used by Sandradewi et al.<sup>10</sup> to quantify the mass fractions of total carbonaceous matter from wood burning and traffic emissions at a certain wavelength. Applying this model to the lowest aethalometer wavelength measured in Detling (370 nm), using the biggest wavelength (950 nm),  $\alpha = 1$  and  $\alpha = 2.2$  for traffic and wood burning, respectively, yields the following formula for  $b_{abs}$  at 370 nm due to wood burning carbonaceous matter (S1):

$$b_{abs}(370\text{ nm})_{WB} = \frac{b_{abs}(370\text{ nm}) - \left(\frac{370}{950}\right)^{-1} * b_{abs}(950\text{ nm})}{1 - \frac{\left(\frac{370}{950}\right)^{-1}}{\left(\frac{370}{950}\right)^{-2.2}}} \quad (S1)$$

Figure S9 (hashed bar) shows the classification of the mean  $b_{abs}$  at 370 nm into the wood burning and traffic fraction.

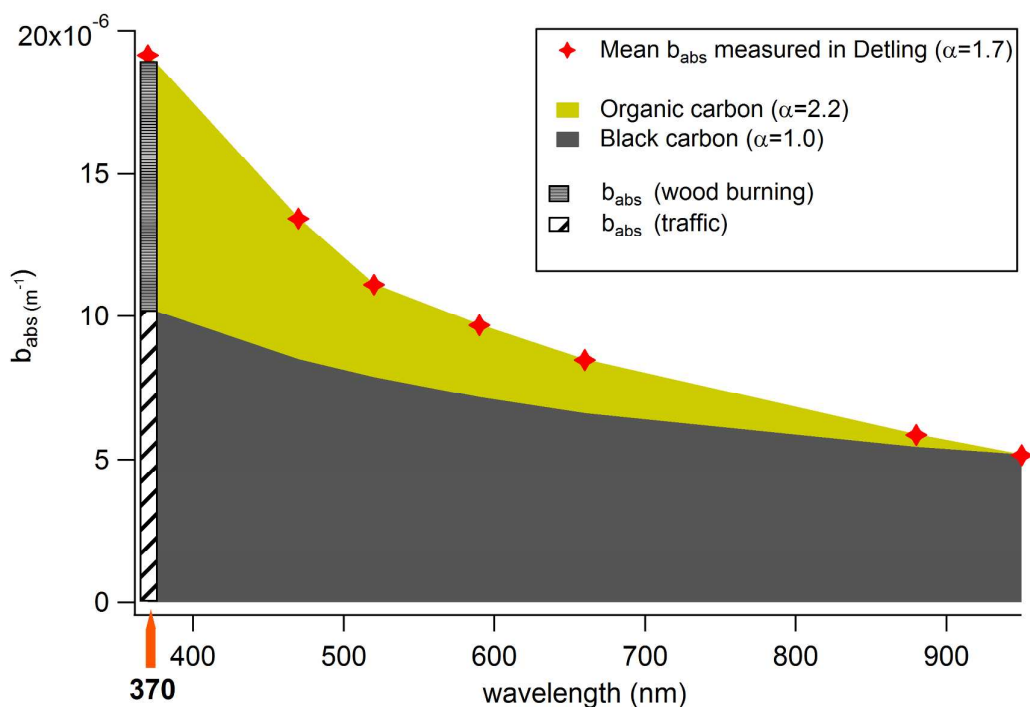


Figure S 9: ClearLo campaign mean values of  $b_{abs}$  as a function of wavelength  $\lambda$  measured by an aethalometer (red 4 point stars). The fraction of  $b_{abs}$  by black carbon (BC) was estimated using the power law relationship between  $b_{abs}$  and  $\lambda$ , and an Angström exponent  $\alpha = 1$  (grey); the fraction of  $b_{abs}$  by organic carbon (green) is the difference between total  $b_{abs}$  and  $b_{abs}(BC)$ , yielding  $\alpha = 2.2$ . The apportionment of  $b_{abs}$  at 370 nm to wood burning (WB) and traffic carbonaceous matter is based on the model developed by Sandradewi et al.,<sup>10</sup> with  $\alpha = 1$  for traffic and  $\alpha = 2.2$  for WB.

## 12. Comparison of absorption measured by the aethalometer and PASS-3

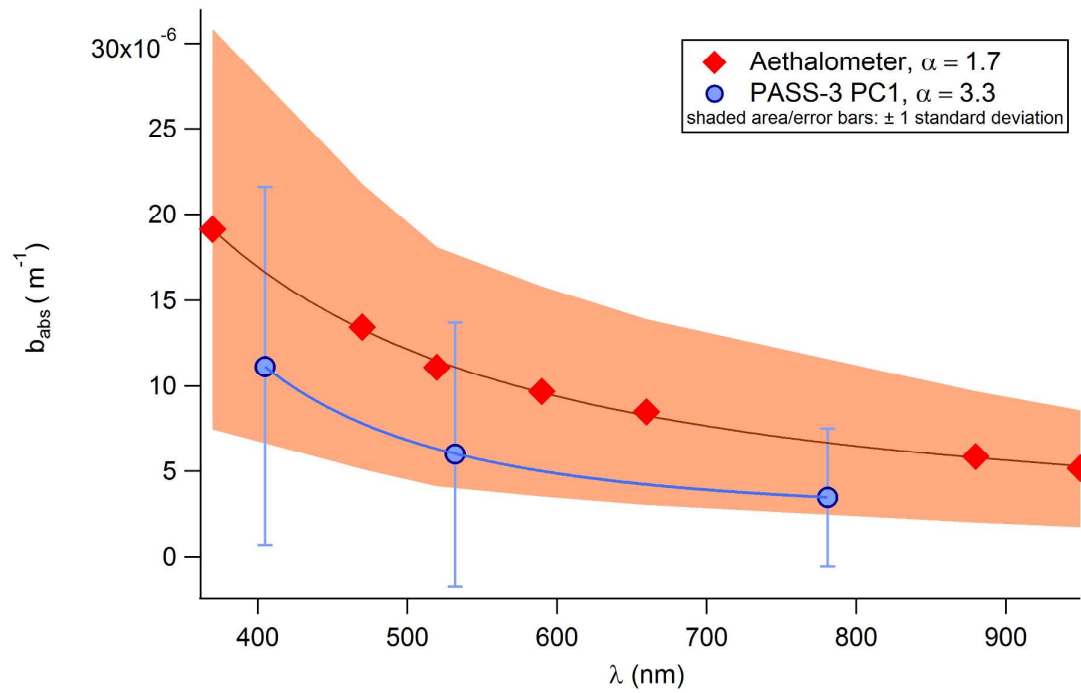


Figure S 10: Comparison of aethalometer and three-wavelength photo-acoustic soot photometer (PASS-3, Droplet Measurement Technologies, USA) light absorption measurements in Detling.

## 13. References

- (1). Department for Environment, F., and Rural Affairs National Atmospheric Emissions Inventory. [naei.defra.gov.uk](http://naei.defra.gov.uk) (09 February 2013),
- (2). Paatero, P. Least squares formulation of robust non-negative factor analysis. *Chemometr. Intell. Lab.* **1997**, *37*, (1), 23-35, DOI 10.1016/S0169-7439(96)00044-5.
- (3). Ulbrich, I. M.; Canagaratna, M. R.; Zhang, Q.; Worsnop, D. R.; Jimenez, J. L. Interpretation of organic components from positive matrix factorization of aerosol mass spectrometric data. *Atmos. Chem. Phys.* **2009**, *9*, (9), 2891-2918, DOI 10.5194/acp-9-2891-2009.
- (4). Allan, J. D.; Delia, A. E.; Coe, H.; Bower, K. N.; Alfarra, M. R.; Jimenez, J. L.; Middlebrook, A. M.; Drewnick, F.; Onasch, T. B.; Canagaratna, M. R.; Jayne, J. T.; Worsnop, D. R. A generalised method for the extraction of chemically resolved mass spectra from Aerodyne aerosol mass spectrometer data. *J. Aerosol. Sci.* **2004**, *35*, (7), 909-922, DOI 10.1016/j.jaerosci.2004.02.007.
- (5). Zhang, Q.; Jimenez, J.; Canagaratna, M.; Ulbrich, I.; Ng, N.; Worsnop, D.; Sun, Y. Understanding atmospheric organic aerosols via factor analysis of aerosol mass spectrometry: a review. *Anal Bioanal Chem* **2011**, *401*, (10), 3045-3067, DOI 10.1007/s00216-011-5355-y.
- (6). Kirchstetter, T. W.; Thatcher, T. L. Contribution of organic carbon to wood smoke particulate matter absorption of solar radiation. *Atmos. Chem. Phys.* **2012**, *12*, (14), 6067-6072, DOI 10.5194/acp-12-6067-2012.
- (7). Kirchstetter, T. W.; Novakov, T.; Hobbs, P. V. Evidence that the spectral dependence of light absorption by aerosols is affected by organic carbon. *J. Geophys. Res-Atmos.* **2004**, *109*, (D21), DOI 10.1029/2004jd004999.
- (8). Schnaiter, M.; Horvath, H.; Mohler, O.; Naumann, K. H.; Saathoff, H.; Schock, O. W. UV-VIS-NIR spectral optical properties of soot and soot-containing aerosols. *J. Aerosol. Sci.* **2003**, *34*, (10), 1421-1444, DOI 10.1016/S0021-8502(03)00361-6.
- (9). Schnaiter, M.; Schmid, O.; Petzold, A.; Fritzsche, L.; Klein, K. F.; Andreae, M. O.; Helas, G.; Thielmann, A.; Gimmler, M.; Mohler, O.; Linke, C.; Schurath, U. Measurement of wavelength-resolved light absorption by aerosols utilizing a UV-VIS extinction cell. *Aerosol. Sci. Technol.* **2005**, *39*, (3), 249-260, DOI 10.1080/027868290925958.
- (10). Sandradewi, J.; Prevot, A. S. H.; Szidat, S.; Perron, N.; Alfarra, M. R.; Lanz, V. A.; Weingartner, E.; Baltensperger, U. Using aerosol light absorption measurements for the quantitative determination of wood burning and traffic emission contributions to particulate matter. *Environ. Sci. Technol.* **2008**, *42*, (9), 3316-3323, DOI 10.1021/es702253m.